IEEE Photonics Journal
An IEEE Photonics Society Publication

Open Access

Temperature Insensitive and Integrated Differential Pressure Sensor for Liquid Level Sensing Based on an Optical Fiber Fabry–Perot Interferometer

Volume 10, Number 4, August 2018

Tiegen Liu
Wanchen Zhang
Shuang Wang
Junfeng Jiang
Kun Liu
Xue Wang
Jinshi Zhang

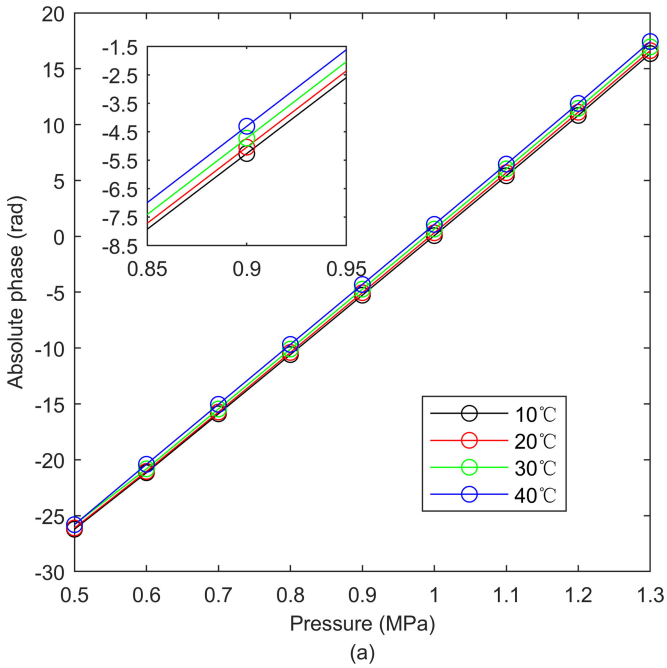

(a)

DOI: 10.1109/JPHOT.2018.2860899
1943-0655 © 2018 IEEE

Temperature Insensitive and Integrated Differential Pressure Sensor for Liquid Level Sensing Based on an Optical Fiber Fabry–Perot Interferometer

Tiegen Liu,[1,2,3] **Wanchen Zhang**,[1,2,3] **Shuang Wang**,[1,2,3] **Junfeng Jiang**,[1,2,3] **Kun Liu**,[1,2,3] **Xue Wang**,[1,2,3] **and Jinshi Zhang**[1,2,3]

[1]School of Precision Instrument and Opto-electronics Engineering, Tianjin University, Tianjin 300072, China
[2]Key Laboratory of Opto-electronics Information Technology, Ministry of Education, Tianjin 300072, China
[3]Tianjin Optical Fiber Sensing Engineering Center, Institute of Optical Fiber Sensing of Tianjin University, Tianjin 300072, China

DOI:10.1109/JPHOT.2018.2860899

Manuscript received May 23, 2018; revised July 22, 2018; accepted July 25, 2018. Date of publication July 27, 2018; date of current version August 13, 2018. This work was supported in part by the National Natural Science Foundation of China under Grants 61505139, 61735011, 61675152, 61775161, 61475114, and 61378043, in part by Tianjin Natural Science Foundation under Grant 16JCQNJC02000, in part by the National Instrumentation Program of China under Grant 2013YQ030915, and in part by China Postdoctoral Science Foundation under Grant 2016M590200. Corresponding authors: Shuang Wang and Junfeng Jiang (e-mail: shuangwang@tju.edu.cn; jiangjfjxu@tju.edu.cn).

Abstract: We propose a temperature insensitive optical fiber Fabry–Perot (FP) sensor for liquid level measurement. The sensor is based on a silicon diaphragm and borosilicate glass ferrules. Through the combination of different ferrules, the FP cavity is fabricated without a seal to eliminate the influence of the residual air in the FP cavity, thereby the temperature cross-sensitivity is significantly reduced. The opened FP cavity constitutes a differential pressure sensing structure at the same time. To verify the performance of this sensor, an experiment with an optical fiber pressure and temperature experiment system is carried out. The measuring range is 0.5–1.3 MPa. The sensor has a good monotonic linear response with an accuracy less than 0.4% F.S. (full scale). The measuring error caused by the temperature drift is lower than 0.0007 MPa/K, i.e., 0.09% F.S./K.

Index Terms: Optical fiber sensors, optical fibers, pressure sensors, altimetry.

1. Introduction

Nowadays, liquid level measurement plays an indispensable role in industrial and daily-life applications. We need to measure the liquid level in many application situations [1], such as dams, water supply systems, oil wells, oil tanks and so on. Traditional electrical sensors are difficult to meet the requirements of liquid level measurement under the harsh environment of conductive, flammable and strong corrosion because of the material of the sensor [2]. Compared with electrical sensors, optical fiber sensors are resistant to electromagnetic interference, uninflammable and resistant to corrosion.

With the development of optical fiber sensing technology, many kinds of optical fiber sensors have been proposed to achieve liquid level measurements. Some sensors transform the liquid level

changing into the refractive index changing, such as sensors based on no-core fiber [3], glass prism [4], and optical fiber itself [5]. Some sensors measure the liquid level by measure the strain on the sensors, such as sensors based on long-period grating [6], [7], fiber Bragg grating [8], [9], and tilt fiber Bragg grating [10], [11]. The sensor based on no-core fiber has a good monotonic linear response, but its measurement range is limited by the length of no-core fiber. The sensor based on glass prism is hard to be used in continuous liquid level measurement. The sensors based on optical fiber itself and fiber gratings are sensitive to the temperature and difficult to be applied to liquid level measurement when temperature changing if no temperature compensation sensor exist. For example, a liquid level sensor based on a polymer optical fiber Bragg grating presented by Marques has a temperature sensitivity of 1.333% F.S./K [12]. Besides, unlike the sensors mentioned above, some sensors transform the liquid level changing into the liquid pressure changing, such as sensors based on Fabry-Perot interference (FPI) [13]. The FPI sensor with a diaphragm as a reflector of the Fabry-Perot (FP) cavity is an effective sensor in liquid level measurement. However, it is difficult to avoid leaving residual gas in a closed structure FP cavity during the fabrication process. The residual gas will cause an undesirable pressure on the diaphragm and weakens the temperature stability of the sensor [14]. Meanwhile, when we use the closed structure FP sensors in liquid level measurement, the pressure on the outside surface of the diaphragm is the pressure of the liquid and the air above it, in other words, air pressure affects the liquid level measurement. In 2014, Wang [15] presented an optical fiber FPI sensor by using the gap between fiber and ferrule as a vent hole, however, the sensor showed large nonlinear response and experimental measure range is only 50 kPa. Tiny diameter difference between fiber and ferrule hole will hinder rapid response of the sensor because of large fluid resistance and deteriorate further under the dirty environment. In addition, the sensor is difficult to fabricate and single fiber fixing point make the sensor fragile.

In this paper, a FPI liquid level sensor based on a silicon diaphragm and borosilicate glass ferrules is proposed and demonstrated. Through the combination of different ferrules, the FP cavity is opened to eliminate the influence of residual gas and thereby the temperature cross-sensitivity is significantly reduced. The opened FP cavity constitutes a differential pressure sensing structure at the same time. No heating is involved in the manufacturing process. To verify the performance of this sensor, an experiment with an optical fiber pressure and temperature experiment system is carried out. The measuring range is 0.5–1.3 MPa. The sensor has a good monotonic linear pressure response and the measuring error caused by the temperature drift is lower than 0.0007 MPa/K, i.e., 0.09% F.S./K.

2. Theory and Sensor Design

Fig. 1. shows the basic structure of an extrinsic FPI pressure sensor. The end face of the optical fiber and the inner surface of the diaphragm are the two reflectors of the FP cavity. A part of the light in the fiber is reflected at the end face of the fiber to form a reflected reference light. Another part of the light propagates to the inner surface of the diaphragm, reflects and forms a reflection sensing light. The reflection sensing light is coupled into the fiber and overlaps with the reflection reference light to form interference light signal. We can get information of the FP cavity length L by demodulating the interference light signal which propagates back to the detector through the fiber.

When the liquid pressure which applies on the diaphragm changes, the deflection of the diaphragm changes. The change of the deflection makes the L and the interference signal change. When the radius and thickness of the diaphragm adapt to the thin plate approximation condition, the deflection ω of the center of the diaphragm can be expressed as [16]

$$\omega = \frac{3a^4\left(1-\gamma^2\right)}{16Ed^3}P \tag{1}$$

where a, d, P, γ, E represent radius, thickness, pressure difference, Poisson's ratio, and Young's modulus of the diaphragm, respectively. Because the pressure sensitivity is in direct proportion to a and inversely proportion to d, choosing big ferrule and thick diaphragm can make the sensor more sensitive to the pressure.

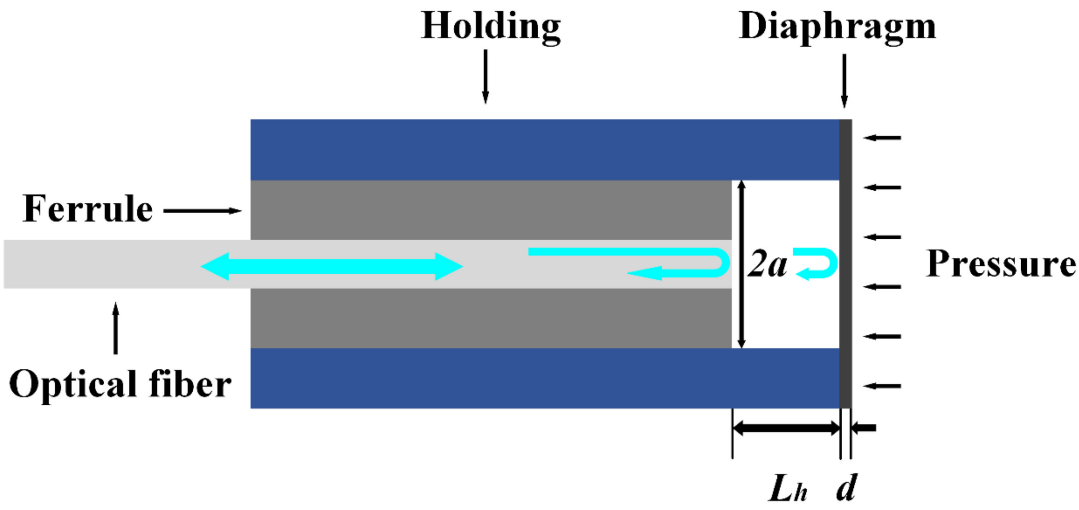

Fig. 1. Structure of an extrinsic FPI pressure sensor.

Fig. 2. An extrinsic FPI pressure sensor with a vent.

If the FP cavity is hermetically sealed, there is easy to be residual gas in the cavity during the manufacturing process. As described above, the ω depends on the pressure difference on the two side of the diaphragm. The pressure difference also can be described as the difference between the pressure of the residual gas and the pressure being measured. Furthermore, the pressure of the residual gas depends on the temperature and the volume of the cavity. So the ω can be expressed as

$$\omega = \frac{3a^4\left(1-\gamma^2\right)}{16Ed^3}\left(P - P_{r(P,V,T,P_{r0})}\right) \tag{2}$$

where P, P_r, V, T, P_{r0} represent the liquid pressure, the pressure of the residual gas, cavity volume, temperature, and the original pressure of the residual gas when the sensor is being fabricated, respectively.

When we slot the ferrule of the sensor in Fig. 1., the FP cavity will be non-enclosed (shown in Fig. 2.). The pressure in the cavity can be treated as invariant. In this consequence, the dominant factors of the temperature sensitivity are the thermal expansion and the temperature sensitivity of the Young's modulus. In the model of the sensor mentioned above, the FP cavity length L can be expressed as

$$L = L_h - \omega \tag{3}$$

where L_h represents the length of the holding, shown in Fig. 1.

To get the expression of the temperature sensitivity of the Young's modulus and the material's expansion, differentiate both sides of the equation.

$$\Delta L = \Delta L_h - \Delta\omega \tag{4}$$

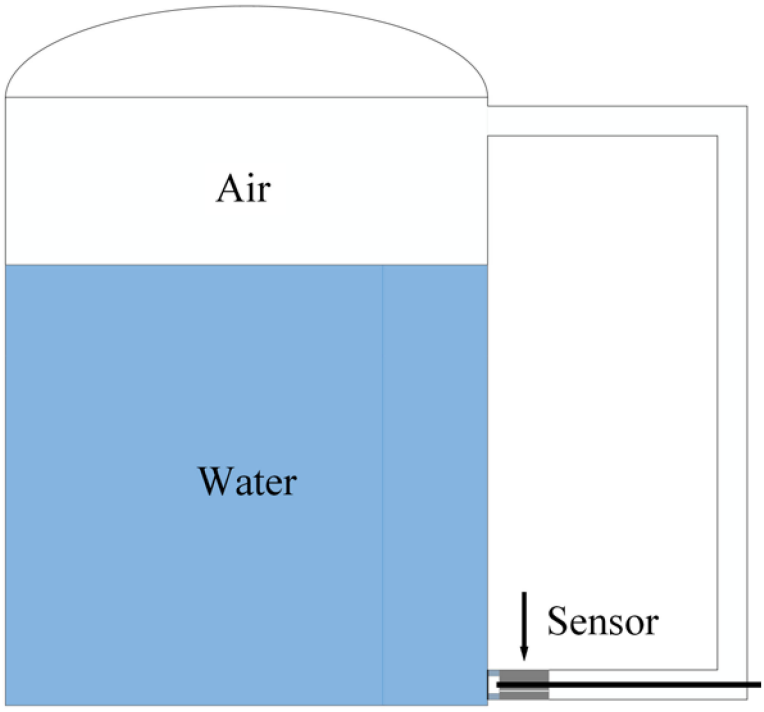

Fig. 3. Sensor set in a container.

here ΔL represents the cavity length change caused by the temperature, ΔL_h and $\Delta\omega$ can be expressed as

$$\begin{aligned}\Delta L_h &= \alpha_h L_h \Delta T \\ \Delta\omega &= \frac{3a^3(1-\gamma^2)}{4Ed^3}P\cdot\Delta a - \frac{9a^4(1-\gamma^2)}{16Ed^2}P\cdot\Delta d - \frac{3a^4(1-\gamma^2)}{16d^3}P\cdot\Delta E \\ &= \omega\left(4\frac{\Delta a}{a} - 3\frac{\Delta d}{d} - \frac{\Delta E}{E}\right)\end{aligned} \tag{5}$$

What's more, Δa, Δd, ΔE can be expressed as $\Delta a = \alpha_\omega a\Delta T$, $\Delta d = \alpha_\omega d\Delta T$, $\Delta E = \beta_\omega E\Delta T$, where α_h, α_ω, β_ω represent the linear thermal expansion coefficient of the holding, diaphragm, and the young's modulus temperature coefficient of the diaphragm, respectively. Equation (4) changes to

$$\Delta L = \alpha_h L_h \Delta T - \omega(\alpha_\omega \Delta T - \beta_\omega \Delta T) \tag{6}$$

At room temperature, α_h, α_ω, β_ω are $3.3 * 10\hat{} - 6/\mathrm{K}, 2.3 * 10\hat{} - 6/\mathrm{K}$, and $-64.73 * 10\hat{} - 6/\mathrm{K}$, respectively. As these coefficient are in magnitude of $10\hat{}{-}5$, the temperature sensitivity of the sensor is extremely low.

Meanwhile, when we set this kind of sensor in a container (shown in Fig. 3.), on the one side of the diaphragm, the pressure is the liquid pressure and the air pressure in the container, on the other side of the diaphragm, the pressure is the air pressure in the container. As a result, the pressure difference on the two side of the diaphragm represent the liquid pressure. We integrate the traditional differential pressure sensors together and make the structure simple.

3. Experiment, Results and Discussion

We bring in a D-shape ferrule to achieve the sensor structure mentioned in Fig. 2(a). The schematic diagram of the sensor is showed in Fig. 4. The D-shape ferrule and the bigger ferrule form a vent.

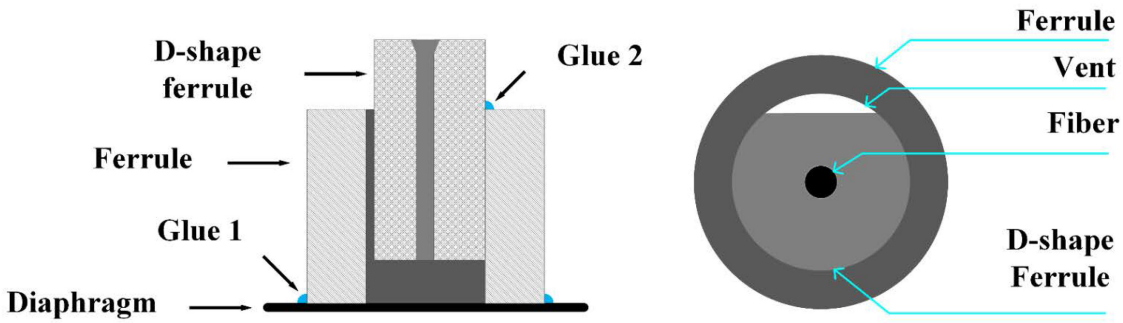

Fig. 4. The schematic diagram of the sensor.

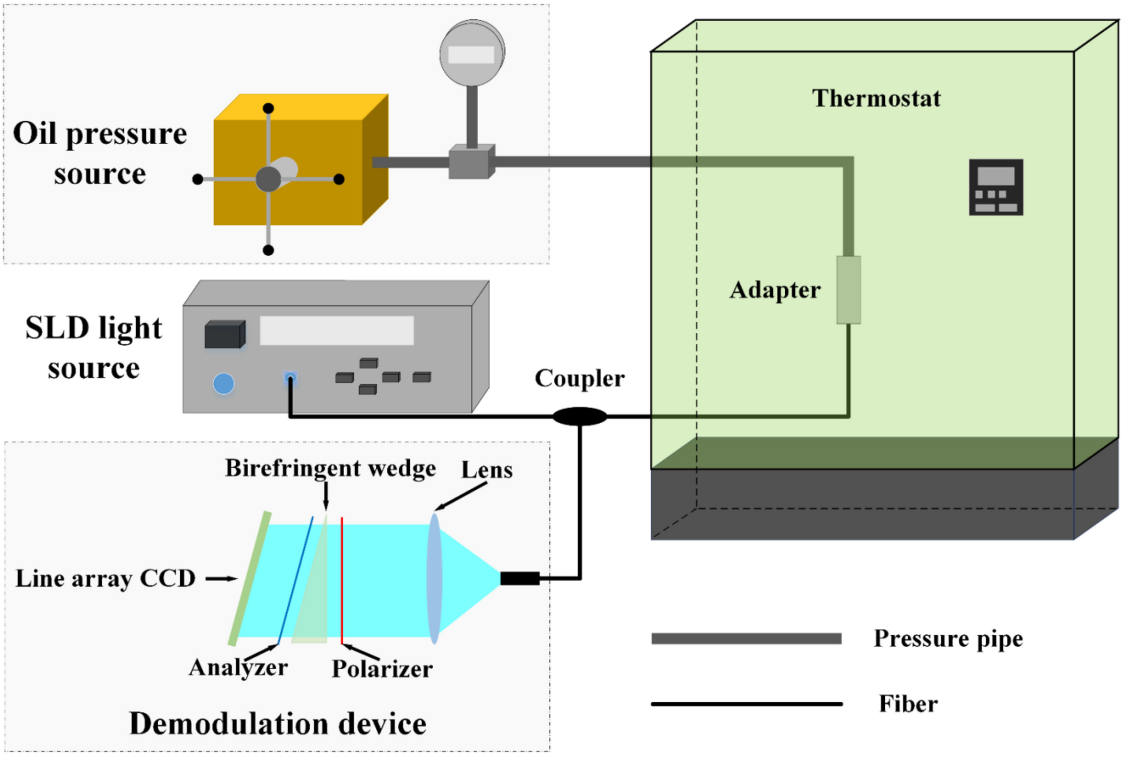

Fig. 5. The schematic diagram of pressure and temperature experiment equipment.

The sensor is fabricated without laser weld or other heating process, therefore the thermal stress can be ignored and will not weaken the temperature stability of the sensor. To make a contrast, we fabricate two sensors, one is fabricated as Fig. 4 shows (named 'vent sensor') and the other one is hermetically sealed by blocking off the vent using excess glue (named 'no vent sensor').

The thickness of the diaphragm is 100 μm. The external diameter and inner diameter of the ferrule is 4.5 mm and 2.51 mm, respectively. The external diameter and inner diameter of the D-shape ferrule is 2.5 mm and 0.126 mm, respectively. The flat part of the D-shape is 1.6 mm wide. By Equation (1) we can get that the ω is 1.6 μm and 4.2 μm when the pressure is 0.5 MPa and 1.3 MPa, respectively. The theoretical pressure sensitivity is 3.2 μm/MPa.

Fig. 5 shows the schematic diagram of the pressure and temperature experiment equipment. The light source with a central wavelength of 1550 nm is generated by a superluminescent diode (SLD) light source and propagates to the FP cavity of the sensor through the single model fiber and the

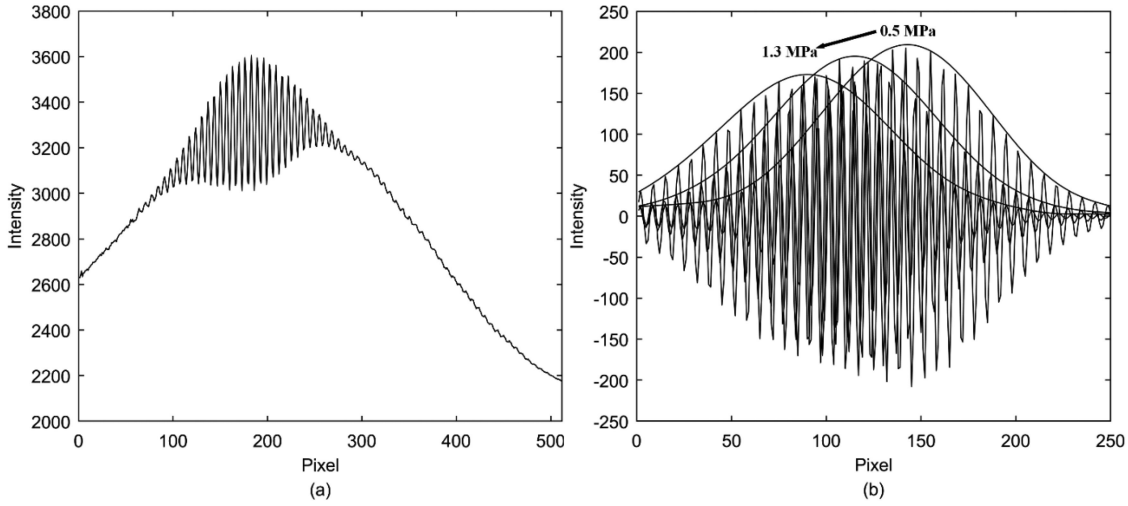

Fig. 6. (a) The original signal. (b) The signal after shaped.

optical circulator. The interference signal propagates back to the demodulation device through the fiber and the circulator.

The core of the demodulation device is a spatial-scan type demodulation system which is based on polarization low coherence interference [17]. The interference signal propagates through the lens, polarizer, birefringent wedge, analyzer and illuminates the line array CCD. The polarization directions of the polarizer and the detector are perpendicular to each other and are 45 degrees with the optical axis of the birefringent optical wedge. Thus the light signal in the birefringent wedge is divided into two beams with different refractive index and different optical path. These two beams overlap together at the analyzer and form an interference signal. When the optical path difference in the birefringent wedge is equal to the optical path difference produced by the FP cavity, there will be low coherent interference fringes on the CCD. By determining the peak position of the interference fringes, we obtain the absolute phase of the interference signal. As the absolute phase corresponds to the FP cavity length, we can use the absolute phase to measure the pressure [18].

The sensor is placed inside of a thermostat and connected to the pressure source by pressure pipe and adapters. The pressure is provided by an oil pressure source whose pressure is adjusted manually.

When experiment is in progress, first, set the temperature of the thermostat and wait to keep the temperature steady (about 1 hour). Second, boost the pressure to 0.5 MPa and wait to keep the pressure steady (about 10 minutes). Third, capture the signal of the CCD in the demodulation device. Then increase the pressure by 0.1 MPa and capture the signal again until the pressure is 1.3 MPa.

Fig. 6(a) shows the original signal get by the CCD when the fiber is fixed in the D-shape ferrule. Fig. 6(b) shows the experimental signals of 0.5, 0.9, 1.3 MPa which have been reshaped. When the pressure increases, the deflection ω increases and the FP cavity length L decreases. As a result, low coherence interference fringes on the CCD moves from right side to left side unidirectionally.

Fig. 7(a) shows the absolute phase-pressure curve of the vent sensor under several different temperature conditions. Under several different temperature conditions, the absolute phase and pressure of the vent sensor have a good monotonic linear relationship (coefficient of determination $R^2 \geq 0.9999$). The full range measurement accuracy of the vent sensor is within 0.4% F.S. Fig. 7(a) shows that, when temperature raises, the demodulated absolute phase at each pressure increases, which means the cavity length L decreases. Fig. 7(b) shows the temperature drift of the vent sensor using the absolute phase of 10 °C as a reference base. As the measuring range is 0.8 MPa, the measuring error caused by the temperature drift is lower than 0.09% F.S./K. Overall speaking, the measuring error caused by temperature drift increases when the pressure and temperature

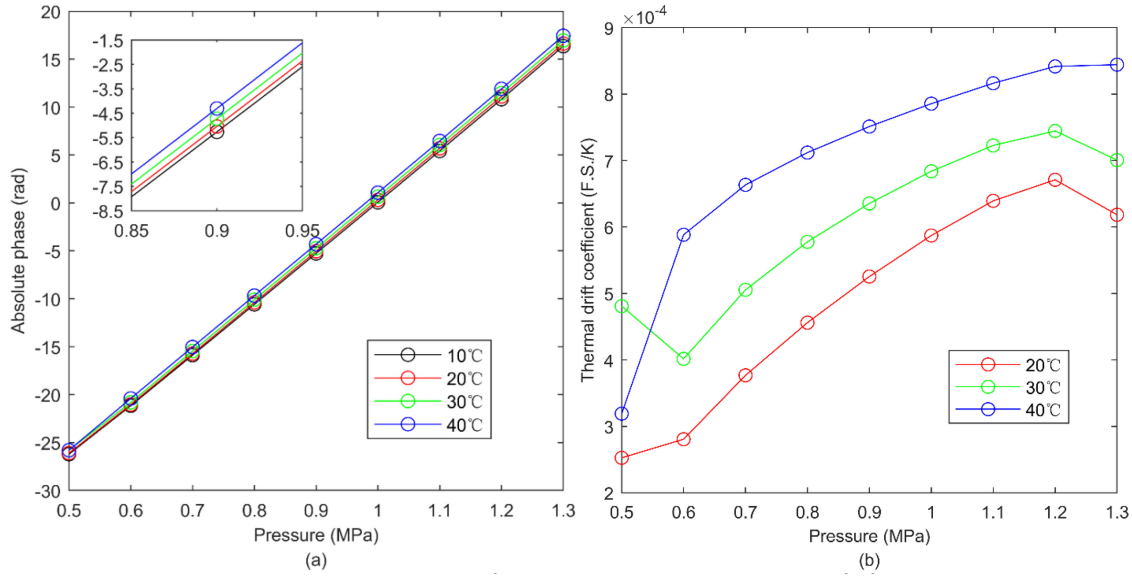

Fig. 7. (a) Absolute phase-pressure curve of the vent sensor. (b) The temperature drift of the vent sensor.

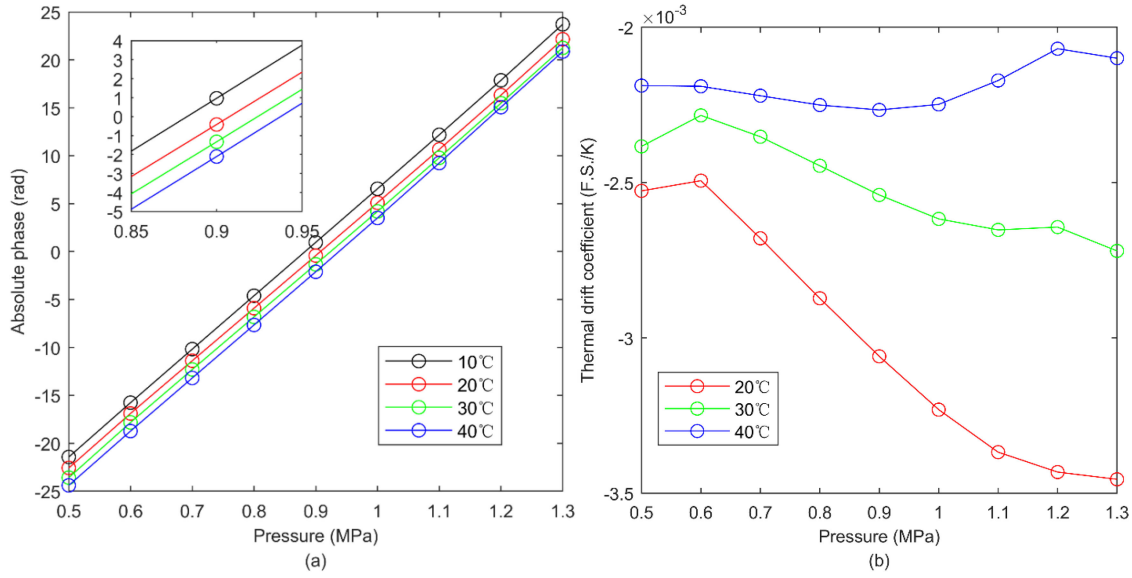

Fig. 8. (a) Absolute phase-pressure curve of the no vent sensor. (b) The temperature drift of the no vent sensor.

increases. This is because in the Equation (4), the cavity length change caused by temperature drift ($-\Delta L$) has positive correlation with the ω and $-\beta_\omega$, while the ω and $-\beta_\omega$ have positive correlation with the pressure and temperature. However, it is obviously larger than the error mentioned in Section 2. We hold the opinion that those glues and hand-made process are the main facts which weaken the temperature stability. When the temperature rises, the glues will expand. As the thermal expansion coefficient of the epoxy glue is larger than that of the silicon diaphragm, which is about $6 * 10\hat{}-5$, the glue will squeeze the silicon diaphragm, cause additional deformation.

Fig. 8 shows the absolute phase-pressure curve and the temperature drift of the no vent sensor. Fig. 8(a) shows that the no vent sensor has an opposite temperature drift direction compared with the vent sensor. Fig. 8(b) shows that the temperature drift coefficient is negative and its absolute

value is obviously larger than that of the vent sensor, as the gas enclosed in the sensor weakens the temperature stability and make a more complicated relationship with the temperature.

4. Conclusion

In conclusion, we propose a temperature insensitive optical fiber Fabry-Perot (FP) sensor for liquid level measurement. The sensor is made of silicon diaphragm and borosilicate glass ferrules. The FP cavity is fabricated without a seal to eliminate the influence of the residual air in the cavity and form a differential pressure sensor structure. In pressure and temperature experiment, the measuring range is 0.5–1.3 MPa. The sensor has a good monotonic linear pressure response with a measurement accuracy within 0.4% F.S. The measuring error caused by the temperature drift is lower than 0.09% F.S./K. By change the parameters of the silicon diaphragm, we can achieve different range of pressure measurements. The sensor is easier to fabricate and its large vent hole can help to ensure rapid response of the sensor and prompt its adaptability to dirt enviroment. This sensor has significant potential applications in liquid level sensing.

References

[1] A. Cataldo, E. Piuzzi, E. De Benedetto, and G. Cannazza, "Experimental characterization and performance evaluation of flexible two-wire probes for TDR monitoring of liquid level," *IEEE Trans. Instrum. Meas.*, vol. 63, no. 12, pp. 2779–2788, Dec. 2014.
[2] B. Jin, X. Liu, Q. Bai, D. Wang, and Y. Wang, "Design and implementation of an intrinsically safe liquid-level sensor using coaxial cable," *Sensors*, vol. 15, no. 6, pp. 12613–12634, 2015.
[3] J. E. Antonio-Lopez, J. J. Sanchez-Mondragon, P. LiKamWa, and D. A. May-Arrioja, "Fiber-optic sensor for liquid level measurement," *Opt. Lett.*, vol. 36, no. 17, pp. 3425–3427, 2011.
[4] H. Golnabi, "Design and operation of a fiber optic sensor for liquid level detection," *Opt. Lasers Eng.*, vol. 41, no. 5, pp. 801–812, 2004.
[5] F. Pérez-Ocón, M. Rubiño, J. M. Abril, P. Casanova, and J. A. Martínez, "Fiber-optic liquid-level continuous gauge," *Sensors Actuators A, Phys.*, vol. 125, no. 2, pp. 124–132, 2006.
[6] S. Khaliq, S. W. James, and R. P. Tatam, "Fiber-optic liquid-level sensor using a long-period grating," *Opt. Lett.*, vol. 26, no. 16, pp. 1224–1226, 2001.
[7] H. Fu *et al.*, "Implementation and characterization of liquid-level sensor based on a long-period fiber grating Mach–Zehnder interferometer," *IEEE Sensors J.*, vol. 11, no. 11, pp. 2878–2882, Nov. 2011.
[8] D. Xiaowei and Z. Ruifeng, "Detection of liquid-level variation using a side-polished fiber Bragg grating," *Opt. Laser Technol.*, vol. 42, no. 1, pp. 214–218, 2010.
[9] C. W. Lai, Y. L. Lo, J. P. Yur, and C. H. Chuang, "Application of fiber Bragg grating level sensor and Fabry-Perot pressure sensor to simultaneous measurement of liquid level and specific gravity," *IEEE Sensors J.*, vol. 12, no. 4, pp. 827–831, Apr. 2012.
[10] A. F. Obaton, G. Laffont, C. Wang, A. Allard, and P. Ferdinand, "Tilted fibre Bragg gratings and phase sensitive-optical low coherence interferometry for refractometry and liquid level sensing," *Sensors Actuators A, Phys.*, vol. 189, pp. 451–458, 2013.
[11] C. Mou, K. Zhou, Z. Yan, H. Fu, and L. Zhang, "Liquid level sensor based on an excessively tilted fibre grating," *Opt. Commun.*, vol. 305, pp. 271–275, 2013.
[12] C. A. Marques, G. D. Peng, and D. J. Webb, "Highly sensitive liquid level monitoring system utilizing polymer fiber Bragg gratings," *Opt. Exp.*, vol. 23, no. 5, pp. 6058–6072, 2015.
[13] T. Lü and S. Yang, "Extrinsic Fabry-Perot cavity optical fiber liquid-level sensor," *Appl. Opt.*, vol. 46, no. 18, pp. 3682–3687, 2007.
[14] T. Liu, J. Yin, J. Jiang, K. Liu, S. Wang, and S. Zou, "Differential-pressure-based fiber-optic temperature sensor using Fabry–Perot interferometry," *Opt. Lett.*, vol. 40, no. 6, pp. 1049–1052, 2015.
[15] W. Wang and F. Li, "Large-range liquid level sensor based on an optical fibre extrinsic Fabry–Perot interferometer," *Opt. Lasers Eng.*, vol. 52, pp. 201–205, 2014.
[16] S. P. Timoshenko and S. Woinowsky-Krieger, *Theory of Plates and Shells*. New York, NY, USA: McGraw-Hill, 1959, pp. 51–55.
[17] S. Wang, T. Liu, J. Jiang, K. Liu, J. Yin, and F. Wu, "Birefringence dispersion compensation demodulation algorithm for polarized low-coherence interferometry," *Opt. Lett.*, vol. 38, no. 16, pp. 3169–3172, 2013.
[18] J. Jiang *et al.*, "A polarized low-coherence interferometry demodulation algorithm by recovering the absolute phase of a selected monochromatic frequency," *Opt. Exp.*, vol. 20, no. 16, pp. 18117–18126, 2012.